ELSEVIER

Materials Science and Engineering A351 (2003) 31–38

MATERIALS SCIENCE & ENGINEERING A

www.elsevier.com/locate/msea

Spark plasma sintering behavior of nanocrystalline WC–10Co cemented carbide powders

Seung I. Cha [a], Soon H. Hong [a,*], Byung K. Kim [b]

[a] *Department of Materials Science and Engineering, Korea Advanced Institute of Science and Technology, 373-1 Kusung-dong, Yusung-gu, Taejon, 305-701, South Korea*

[b] *Korea Institute of Machinery and Materials, 66 Sangnam-dong, Changwon, Kyungnam, South Korea*

Received 15 April 2002; received in revised form 8 August 2002

Abstract

Microstructure and mechanical properties of WC–10Co cemented carbides fabricated by spark plasma sintering (SPS) process were investigated. Nanocrystalline precursor powders were prepared by spray drying process from solution containing ammonia meta-tungstate and cobalt nitrate, and followed by reduction and carbonization into nanocrystalline WC/Co composite powders by a mechano-chemical process. The WC particles of about 100 nm in diameter were mixed homogeneously with Co binder. The nanocrystalline WC–10Co powders were consolidated by SPS process at temperature ranged 900–1100 °C and under a pressure of 50 or 100 MPa, respectively. Optimum consolidation conditions, such as temperature and pressure, were determined by analysing the dimensional changes of powder compact during SPS process. Hardness and fracture toughness of consolidated WC–10Co cemented carbide were measured by using a Vicker's indentation test. The solute content within the Co binder phase of WC–10Co cemented carbide was evaluated by measuring the saturated magnetic moment. It is found that the hardness of cemented carbide was dependent on the density and grain size of WC. The fracture toughness of cemented carbides increased with increasing the saturated magnetic moment, while decreased rapidly when the liquid Co phase was formed during sintering.

Keywords: Spark plasma sintering; Nanocrystalline powders; Cemented carbides; Hardness; Fracture toughness

1. Introduction

During the last several decades, the cemented carbides consisting of WC grains bound with Co phase have been used for cutting tools, rock drill tip and other wear resistant part. The effect of Co composition and the addition of various types of cubic carbides have been investigated to improve the mechanical properties of WC–Co cemented carbides [1]. In recent days, nanocrystalline WC–Co cemented carbides have been fabricated by thermo-chemical and thermo-mechanical process, known as spray conversion process (SCP) [2]. The advantage of SCP is that the WC particle sizes can be reduced below 100 nm. However, the WC grain size in sintered WC–Co cemented carbides becomes much larger than that in pre-sintered powders due to a fast diffusion through liquid phase during conventional liquid phase sintering process. Therefore, even though the initial WC size is less than 100 nm, the grain size increases rapidly up to 500 nm or larger during the conventional liquid phase sintering. Even though the grain growth inhibitors were added in WC–Co, the WC grains size increases up to 300 nm during the liquid phase sintering process [2,3].

The spark plasma sintering (SPS) that enables a powder compact to be sintered by Joule heat and spark plasma generated by high pulsed electric current through the compact has been introduced recently for the sintering of composites, functionally graded materials and nanocrystalline materials. During SPS process, the powder compact could be sintered at a lower temperature than that for conventional sintering because the surface oxides of powders are easily removed by the generated spark plasma [4].

* Correspoding author. Tel.: +82-42-869-3327; fax: +82-42-869-3310

E-mail address: shhong@mail.kaist.ac.kr (S.H. Hong).

0921-5093/02/$ - see front matter
PII: S0921-5093(02)00605-6

In this study, the SPS process to manufacture WC–10Co cemented carbides using nanocrystalline WC–10Co composite powders was investigated. In order to control the grain growth during the SPS process, both the solid state sintering and liquid phase sintering were attempted and the results were compared. The SPS behaviour of nanocrystalline WC–10Co composite powders was compared with that of conventional mixed powders. The hardness and fracture toughness of spark plasma sintered WC–10Co cemented carbides were characterized.

2. Experimental procedure

2.1. Powder preparation

The nanocrystalline WC–10Co composite powders were prepared by SCP from metallic salt containing ammonia meta-tungstate and cobalt nitrate ($Co(NO_3)_2$), and followed by oxidation, reduction and carbonization processes [2]. As shown in Fig. 1, the WC particles of spherical shape were homogeneously dispersed within Co phase in the nanocrystalline WC–10Co composite powders fabricated by SCP. The WC particle sizes were ranged 50–150 nm and the average particle size was measured about 100 nm. The nanocrystalline WC–10Co composite powders were wet ball-milled in ethanol for 24 h. The ball-milled powders were dried in an oven for 24 h at 80 °C. The mixture of conventional WC powders of 1.33 μm and Co powders were wet ball-milled in ethanol for 24 h.

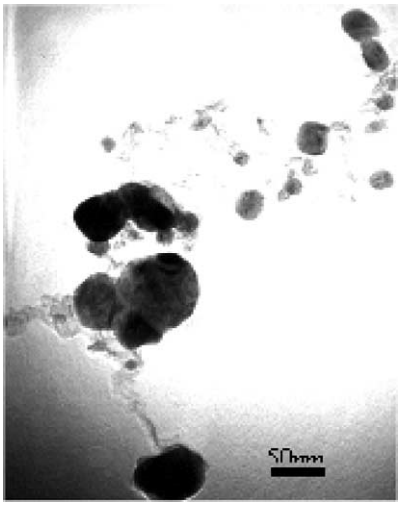

Fig. 1. TEM micrographs of nanocrystalline WC–10Co composite powders fabricated by SCP. The darker phase represents WC phase with average diameter of 100 nm and the brighter phase represent Co phase.

2.2. Consolidation process

The prepared nanocrystalline WC–10Co composite powders and the mixed powders of conventional WC and Co were consolidated by SPS system produced by Sumitomo Coal Mining Co. Ltd. The schematic of SPS system was shown in Fig. 2. In SPS process, the powders in the graphite mould were heated by applied pulsed electric current of 1000 A. The pressure was applied with the current. The powders were sintered by heat, generated by Joule heating and impedance within the powders generated by pulsed current, and pressure. Specimens with diameter of 15 mm and thickness of 7 mm were densified by the SPS for 10 min at temperature ranged from 900 to 1100 °C under a pressure of 50 or 100 MPa, respectively, in vacuum. The heating rate was maintained as 100 °C min^{-1}. The compact was held at 600 °C for 5 min to remove the organic impurities such as dust and ethanol.

During the consolidation process, the dimensional changes of powders were monitored by measuring the position of lower ram in Fig. 2, which plays a role of electrode to produce high pulsed current within the powder compact and, at the same time, press to apply. The consolidation mechanism, i.e. liquid phase sintering or solid state sintering, is determined by the dimensional changes according to processing temperature as shown in Fig. 3. When the liquid phase was formed during the SPS, the volume of sintered body slightly increased due to the larger volume of liquid Co compared to that of solid as shown in Fig. 3(b). If liquid phase is not formed during the sintering process, the dimension of powder compact decreases continuously by densification. The formation of liquid phase was observed at lower temperature of 1050 °C for nanocrystalline composite powders, while observed at 1100 °C for conventional mixed powders.

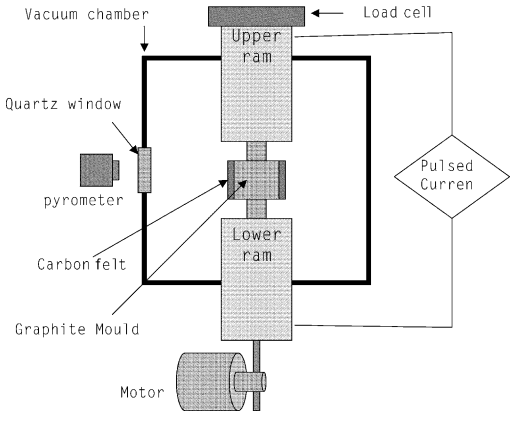

Fig. 2. Schematics of SPS system used for consolidation of WC–10Co cemented carbides.

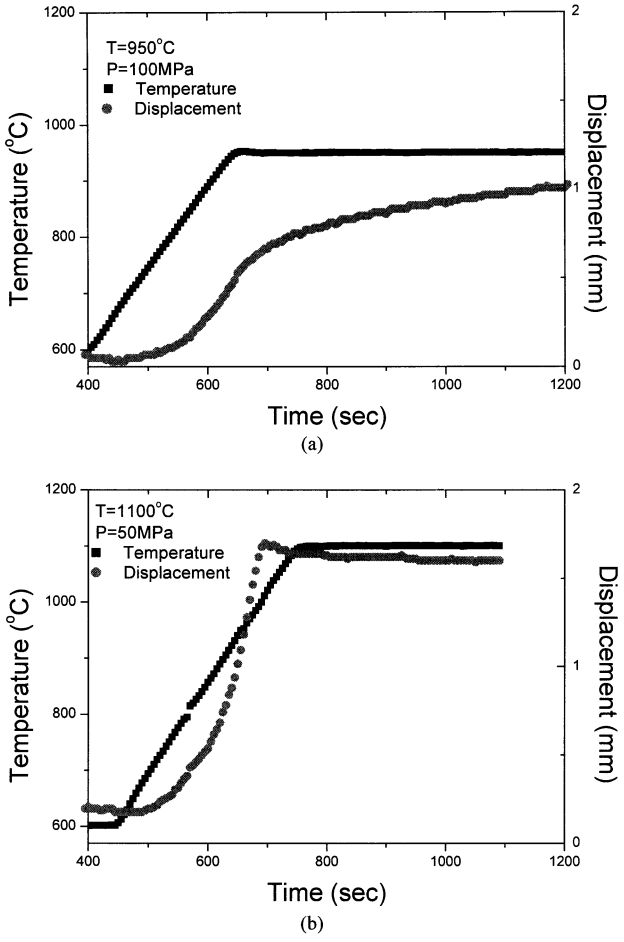

Fig. 3. The variation of temperature and displacement during SPS of nanocrystalline WC–10Co cemented carbide powders; (a) solid state sintering at set temperature of 950 °C, (b) liquid phase sintering at set temperature of 1100 °C. The positive sign of displacement indicates the shrinkage of specimen during the SPS.

2.3. Characterization of sintered WC–Co

The microstructure of sintered WC–Co cemented carbides was observed by the scanning electron microscope (SEM) and the optical microscope. Solute concentration within the Co binder phase was analyzed by measuring the saturated magnetic moment of WC–10Co cemented carbides. In general, the saturated magnetic moment of WC–Co cemented carbides was dependent on content of W within the Co binder phase as follows [5],

$$4\pi M_s = 4\pi(S_0 - PC_W) \quad (1)$$

where S_0 is saturated magnetic moment of pure Co, P is constant ranged 0.8–1.06 and C_W is atomic content of W in Co binder phase.

Hardness was measured by Vicker's hardness tester under a constant load of 9.8 N. The fracture toughness of WC–Co cemented carbides was determined by measuring the crack length near the indent made by Vicker's indentation load of 98 N (10 kgf) and calculated by using the following equation [7],

$$K_{IC} = 0.016\sqrt{\frac{E}{H}}\left(\frac{P}{L}\right)^{1.5} \quad (2)$$

where K_{IC} is fracture toughness of cemented carbides, E is Young's modulus of cemented carbides, H is hardness of cemented carbides, P is indentation load and L is crack length near the indent. The Young's modulus of cemented carbides, E, is generally known as about 611 GPa according to the rule of mixture calculation between Young's modulus of WC and pure Co [8,9]. Young's modulus of Co binder phase could be varied with W and C content alloyed during liquid phase sintering process and it could affect the Young's modulus of cemented carbides. However, in this study, the composition of cemented carbides is WC–10 wt.% Co and it contains about 84 vol.% of WC and 16 vol.% Co binder phase. Furthermore, the Young's modulus of WC is about 696 GPa and this value is much larger than that of Co whose Young's modulus is about 174 GPa [10,11]. Even though the W and C content varied from 0% to saturated values, the Young's modulus of WC–10Co cemented carbides varied from 611 to 620 GPa according to the rule of mixture calculation. Therefore, the effect of difference in Young's modulus owing to the W and C content within Co binder phase on fracture toughness is much small and can be neglected. In this study, the Young's modulus of cemented carbides is considered as 611 GPa which is generally accepted as Young's modulus of cemented carbides [8,9].

The cracks induced by Vicker's indentation were shown in Fig. 4. The cracks were sharp and straight

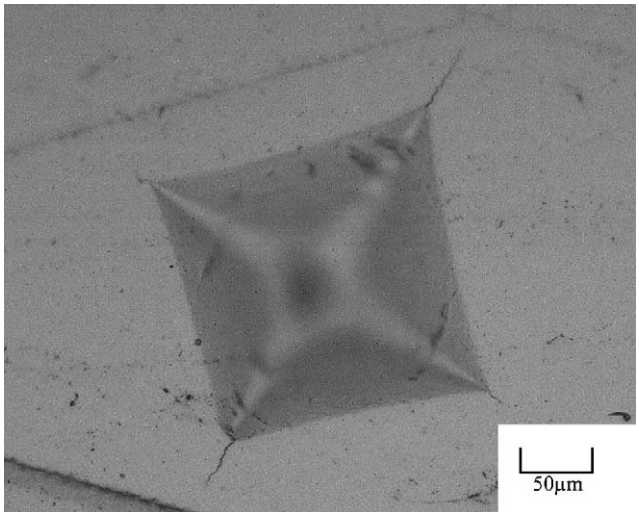

Fig. 4. Optical micrographs of cracks induced by Vicker's indentation on cemented carbides spark plasma sintered from nanocrystalline WC–10Co at 1050 °C under 50 MPa.

enough to measure the fracture toughness by measuring the length of crack induced by Vicker's indentations.

3. Results and discussion

3.1. Densification behaviour and microstructure

The densification behaviour and the grain size of WC–10Co cemented carbide sintered at various temperatures were shown in Fig. 5(a) and (b), respectively. The density of the WC–10Co cemented carbide increased with increasing the sintering temperature. The WC–10Co cemented carbide sintered from nanocrystalline composite powders showed full densification at lower temperature compared to the conventional mixed powders. When the sintering was performed under higher pressure, higher density was obtained at lower sintering temperature. The grain size increased slightly with increasing the sintering temperature during solid state sintering, while increased rapidly with increasing the sintering temperature when the liquid Co phase was formed as shown in Fig. 5(b). When the nanocrystalline WC–10Co composite powders solid state sintered at

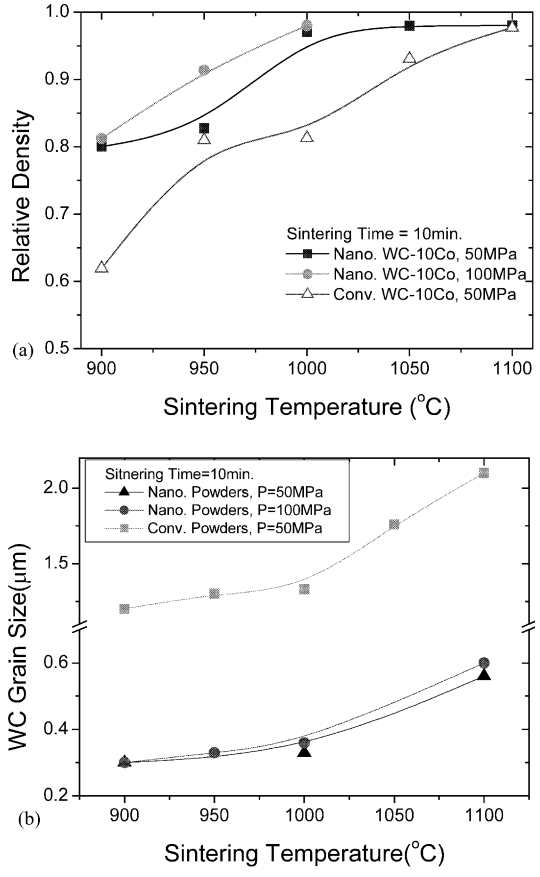

Fig. 5. The variation of (a) relative density and (b) WC grain size in sintered WC–10Co with varying the SPS temperature of nanocrystalline and conventional WC–10Co powders.

1000 °C by SPS process, a full densification of WC–10Co could be obtained with little grain growth of WC as shown in Fig. 5(a) and (b), respectively. The average WC grain size was about 300 nm with full densification if spark plasma sintered at 1000 °C, while increased over 600 nm if spark plasma sintered at temperature for liquid phase sintering. The grain size of WC spark plasma sintered at 1000 °C is much smaller than that of conventional liquid phase sintered [3], even though the initial WC size of the powders were almost the same.

The microstructure of sintered WC–10Co cemented carbide was also dependent on the initial powder conditions. In case of sintering of nanocrystalline composite powders, the liquid phase was not formed during SPS process up to 1000 °C and melting of Co binder phase started from 1050 °C under pressure of both 50 and 100 MPa. As shown in Fig. 6, a group of small pores were observed in WC–10Co cemented carbide sintered at 900 °C. However, the small pores disappeared rapidly and spherical shaped large pores were only observed as increasing the SPS temperature. The elimination of the pores occurred at the temperature of 1000 °C, which is below the liquid Co binder phase formed, hence the WC–10Co cemented carbide was fully densified by solid state sintering. It was found from SEM observations in Fig. 6 that the WC grains were round shape, like initial WC shape within the nanocrystalline WC–10Co composite powders, when spark plasma sintered at 900 °C. When the sintering temperature was 1000 °C, the faceted and round WC grains were mixed in spite of no Co liquid phase formed. Fully faceted WC grains were observed in WC–10Co cemented carbides liquid phase sintered at 1100 °C.

However, in the SPS of conventional mixed powders, the Co necks were formed between WC particles partially at sintering temperature of 900 °C. The region, where Co necks were formed, was densified by solid state sintering, but the region, where Co necks were not formed, remained unfilled with increasing the sintering temperature. The remaining unfilled regions filled by liquid Co binder phase when the temperature increased above the melting point of Co phase as shown in Fig. 7.

3.2. Mechanical properties

The Vicker's hardness of WC–10Co cemented carbide measured under a load of 9.8 N increased with increasing the sintering temperature up to 1000 °C until full densification is obtained as shown in Fig. 8(a). Once a full density was obtained, the hardness decreases with increasing the sintering temperature above 1000 °C due to a grain growth during the sintering.

The fracture toughness, calculated from the crack length induced by the Vicker's indentation test under a load of 98 N, increased with increasing the density of sintered WC–10Co cemented carbide. The fracture

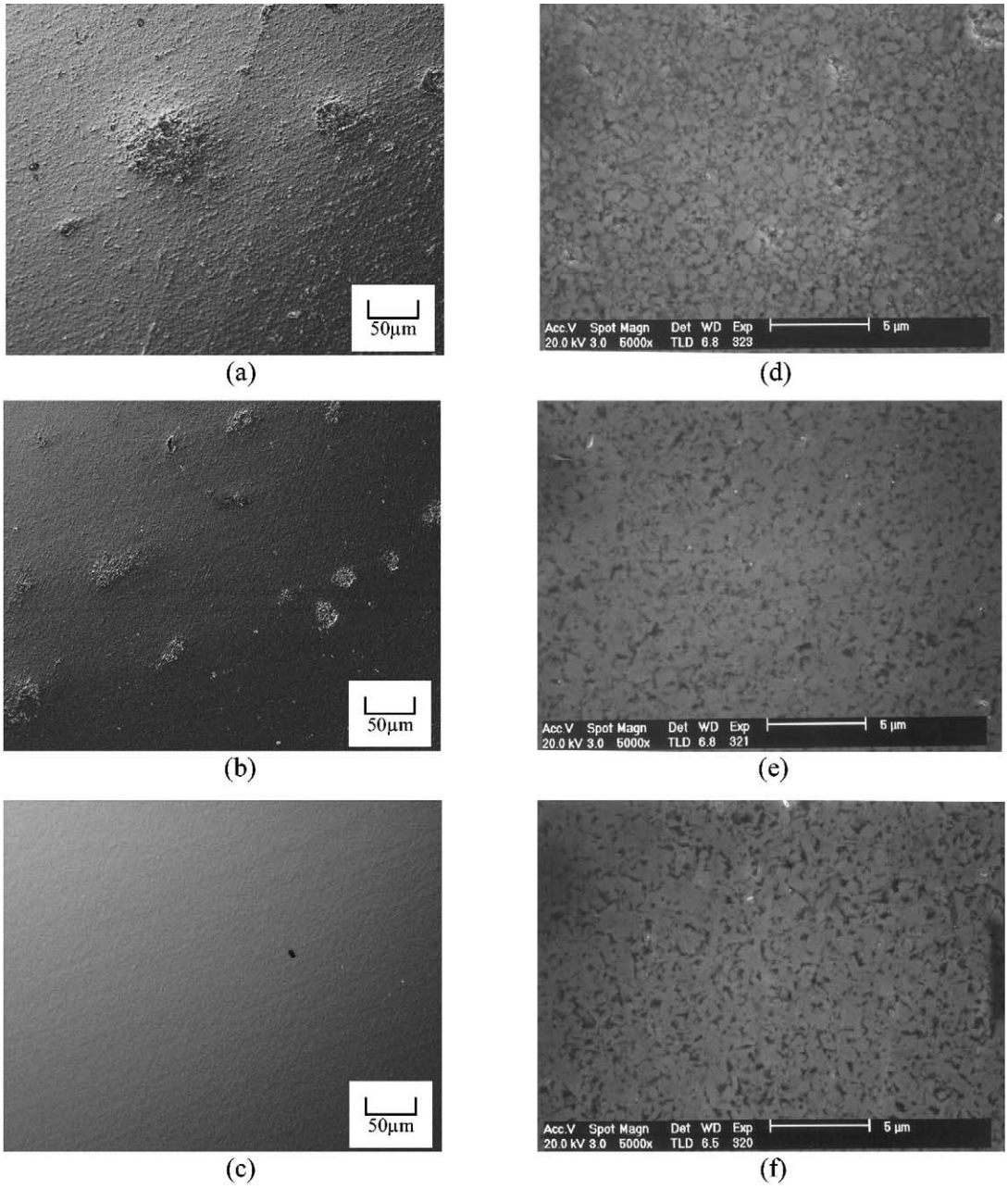

Fig. 6. Optical and scanning electron micrographs of WC–10Co cemented carbides sintered from nanocrystalline WC–10Co powders by SPS under pressure of 50 MPa. Optical micrographs of WC–10Co cemented carbides sintered at (a) 900 °C, (b) 950 °C, (c) 1100 °C, and scanning electron micrographs of WC–10Co cemented carbides sintered at (d) 900 °C, (b) 1000 °C, (c) 1100 °C.

toughness of WC–10Co cemented carbide sintered from the nanocrystalline composite powders were higher than that sintered from the conventional mixed powders. The fracture toughness of WC–10Co cemented carbide sintered from the nanocrystalline composite powders increased with increasing the sintering pressure as shown in Fig. 8(b). However, the fracture toughness of WC–10Co cemented carbide sintered from nanocrystalline composite powders decreased when the liquid Co phase was formed, while those of WC–10Co cemented carbide sintered from the conventional mixed powders did not affected by the formation of liquid phase.

It is noted that the fracture toughness of WC–10Co cemented carbide was sensitively dependent on the saturated magnetic moment of cemented carbides, i.e. W content within the Co binder phase. As shown in the Fig. 9, the saturated magnetic moment of WC–10Co cemented carbide sintered from nanocrystalline composite powders was higher than that of WC–10Co cemented carbide sintered from conventional mixed

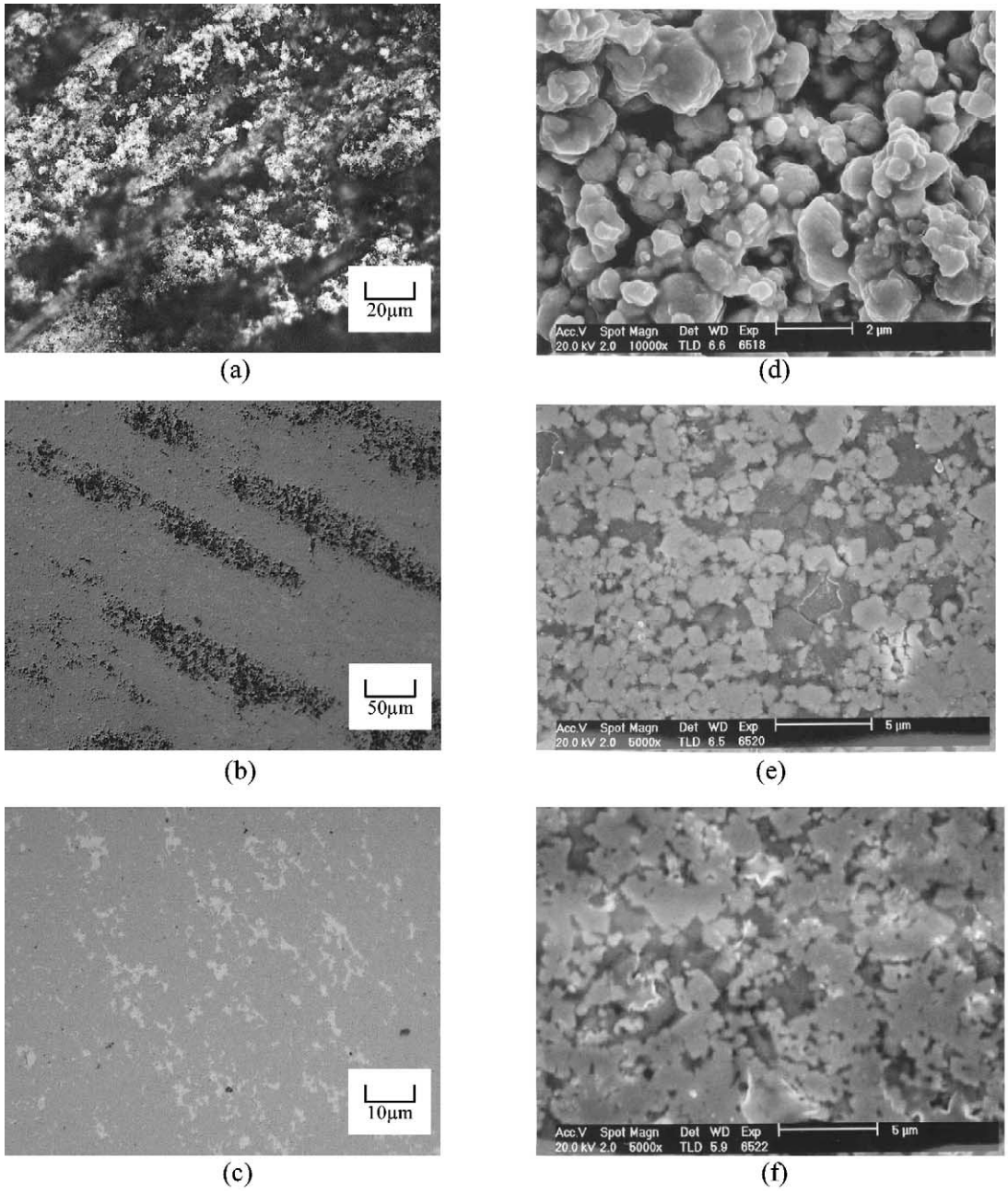

Fig. 7. Optical and scanning electron micrographs of WC–10Co cemented carbides sintered from conventional WC–10Co powders by SPS under pressure of 50 MPa. Optical micrographs of WC–10Co cemented carbides sintered at (a) 900 °C, (b) 1000 °C, (c) 1100 °C, and scanning electron micrographs of WC–10Co cemented carbides sintered at (d) 900 °C, (b) 1000 °C, (c) 1100 °C.

powders before liquid Co phase was formed. When the liquid Co phase was formed during sintering, the saturated magnetic moment of WC–10Co cemented carbide sintered from the nanocrystalline composite powders decreased rapidly, while that of WC–10Co cemented carbide sintered from the conventional mixed powders did not change. From the Fig. 8(b) and Fig. 9, the variation of fracture toughness with varying the sintering temperature was quite similar to the variation of saturated magnetic moment. The dependence of fracture toughness on the saturated magnetic moment was also observed in conventional liquid phase sintered WC–Co cemented carbide [3,12]. However, in case of WC–Co cemented carbide sintered by the conventional liquid phase sintering, the saturated magnetic moment of the conventional cemented carbide was much higher than that of nanocrystalline cemented carbide, and hence the fracture toughness of the conventional WC–10Co cemented carbide was higher than that of the nanocrystalline WC–10Co [13–18].

The saturated magnetic moment of cemented carbide was dependent on the solute content within the Co

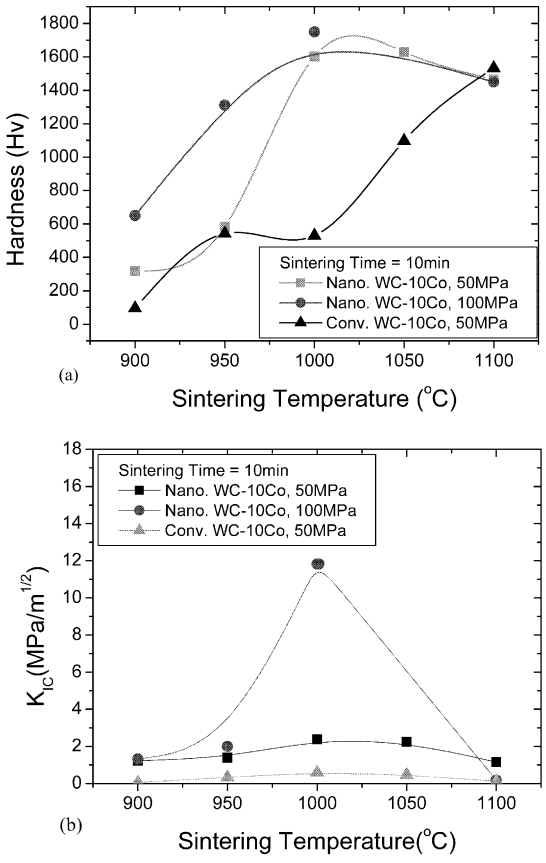

Fig. 8. The variation of (a) hardness and (b) fracture toughness of sintered WC–10Co cemented carbides with varying the SPS temperatures of nanocrystalline and conventional WC–10Co powders.

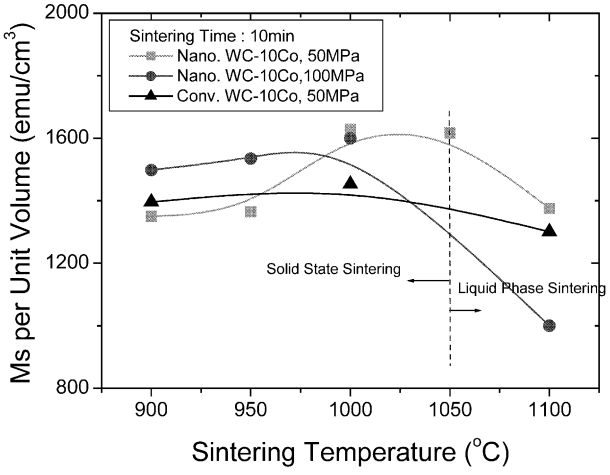

Fig. 9. The variation of saturated magnetic moment per unit volume of Co binder phase of sintered WC–10Co cemented carbides with varying the SPS temperature of nanocrystalline and conventional WC–10Co powders.

binder phase [5]. The dependence of the saturated magnetic moment on the fracture toughness was related to the content of solute atoms such as W and C within the Co binder phase of WC–10Co cemented carbide. The solute atoms of W and C within the Co binder phase influence the mechanical properties of Co binder phase. The Co binder phase in the cemented carbide prevents the crack propagation by shielding a stress field in front of crack tip or by bridging the crack forming ligaments behind the crack tip [13–18]. The crack induced by Vicker's indentation propagates along the Co binder phase as shown in Fig. 10. Therefore, the deformation behaviour of Co binder phase in cemented carbides is the most critical factor determining the fracture toughness of cemented carbides. In solid state sintering temperature, the saturated magnetic moment of WC–10Co cemented carbides sintered from nanocrystalline composite powder is higher than that of WC–10Co cemented carbides sintered from the conven-

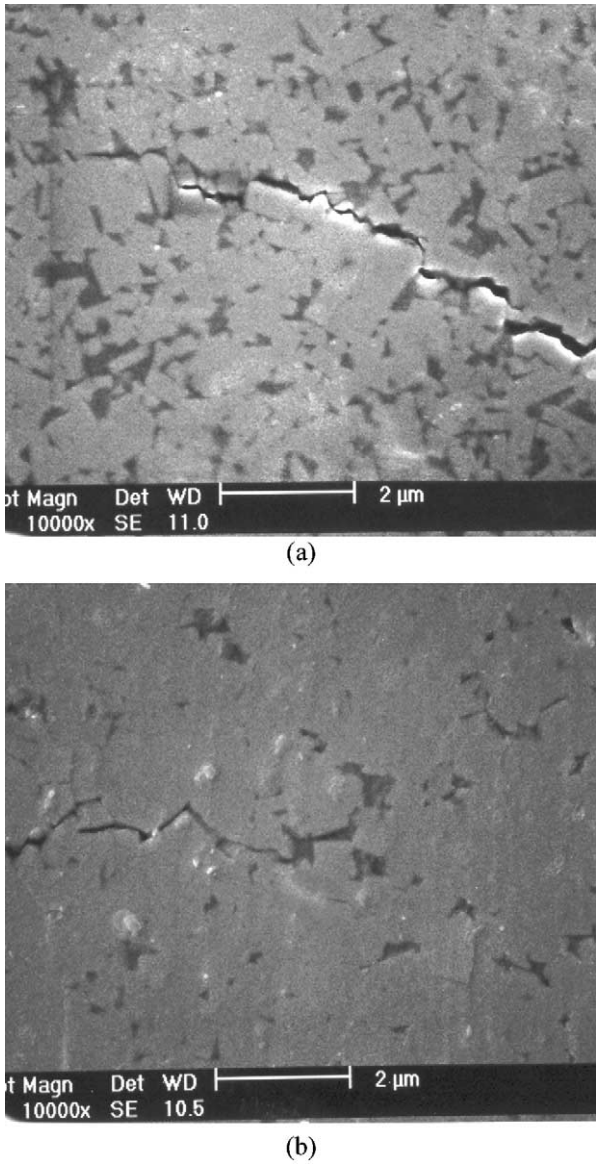

Fig. 10. Microstructures of near the crack tip induced by Vicker's indentation on cemented carbides spark plasma sintered from (a) nanocrystalline WC–10Co powders and (b) conventional WC–10Co powders at 1100 °C under 50 MPa.

tional mixed powders. However the saturated magnetic moment of WC–10Co cemented carbides sintered from the nanocrystalline composite powders decreased more rapidly than that of the conventional one when the liquid phase was formed during sintering. Therefore, if the nanocrystalline WC–10Co powders were liquid phase sintered at high temperature above 1350 °C, the saturated magnetic moment could reduce below that of WC–10Co cemented carbide sintered from conventional mixed powders. It is expected that the higher solubility of W in Co binder phase of the nanocrystalline WC–10Co cemented carbide, when the liquid Co binder phase was formed can be explained by the Gibbs–Thompson effect, in which the solute concentration within the liquid phase increases with decreasing radius of solid during the liquid phase sintering [6].

4. Conclusions

The nanocrystalline WC–10Co composite powders were fully densified by SPS process at the temperature above 1000 °C, which is much lower temperature than that of conventional liquid phase sintering, under a pressure of 50 and 100 MPa. The WC–10Co cemented carbides with WC grain size of 300 nm could be obtained by SPS of nanocrystalline WC–10Co composite powders by solid state sintering process at temperature ranged 950–1000 °C without addition of grain growth inhibitors. While, the conventional mixed WC–10Co powders were spark plasma sintered with full densification only by liquid phase sintering at higher temperature above 1050 °C. The hardness of the sintered WC–10Co cemented carbides was dependent on the grain size of WC. The fracture toughness of solid state sintered WC–10Co cemented carbide was higher than that of liquid phase sintered WC–10Co cemented carbide. The fracture toughness of WC–10Co cemented carbide was significantly influenced by the solute content of W and C in the Co binder phase. This is caused by the modification in deformation behaviour of Co binder phase owing to W and C solute and by the crack path along the Co binder phase.

References

[1] J. Gurland, Int. Mater. Rev. 33 (1988) 151.
[2] B.K. Kim, G.H. Ha, D.W. Lee, J. Mater. Process. Technol. 63 (1997) 317.
[3] Seung I. Cha, Soon H. Hong, Gook H. Ha, Byung K. Kim, Scripta Mater. 44 (8–9) (2001) 1535.
[4] M. Omori, Mat. Sci. Eng. A287 (2000) 183.
[5] B. Roebuck, E.A. Almond, Int. Mater. Rev. 33 (1988) 90.
[6] R.M. German, Sintering Theory and Practice, Wiley, New York, 1996, p. 225.
[7] K. Jia, T.E. Fischer, B. Gallois, Nanostructured Materials 10 (5) (1998) 875.
[8] A.T. Santhanam, P. Tierney, J.L. Hunt, Cemented Carbides, in: ASM Handbook, vol. 7, Powder Metallurgy, ASM International, 1990.
[9] E.K. Storms, The Refractory Carbides, Academic Press, 1978.
[10] G.D. Rieck, Tungsten and its Compounds, Pergamon Press, New York, 1967, p. 387.
[11] W. Betteridge, Cobalt and its Alloys, Ellis Horwood Limited and Wiley, 1982.
[12] S.I. Cha, S.H. Hong, G.H. Ha, B.K. Kim, Int. J. Ref. Met. Hard Mater. 19 (2001) 397.
[13] L.S. Sigl, H.E. Exner, Metall. Trans. A 18A (1987) 1299.
[14] L.S. Sigl, P.A. Mataga, B.J. Dalgleish, R.M. McMeeking, A.G. Evans, Acta Metall. 36 (4) (1988) 945.
[15] A.G. Evans, R.M. MeMeeking, Acta Metall. 34 (12) (1986) 2435.
[16] L.S. Sigl, H.F. Fischmeister, Acta Metall. 36 (4) (1988) 887.
[17] K.S. Ravichandran, Acta Mater. 42 (1994) 143.
[18] M. Kotoul, Acta Mater. 45 (8) (1997) 3363.